

# We are IntechOpen, the world's leading publisher of Open Access books Built by scientists, for scientists

**6,900**

Open access books available

**186,000**

International authors and editors

**200M**

Downloads

**154**

Countries delivered to

**TOP 1%**

most cited scientists

**12.2%**

Contributors from top 500 universities



**WEB OF SCIENCE™**

Selection of our books indexed in the Book Citation Index  
in Web of Science™ Core Collection (BKCI)

Interested in publishing with us?  
Contact [book.department@intechopen.com](mailto:book.department@intechopen.com)

Numbers displayed above are based on latest data collected.

For more information visit [www.intechopen.com](http://www.intechopen.com)



## Chapter

# Effect of M Substitution on Structural, Magnetic and Magnetocaloric Properties of $R_2Fe_{17-x}M_x$ ( $R = Gd, Nd$ ; $M = Co, Cu$ ) Solid Solutions

*Mosbah Jemmali and Lotfi Bessais*

## Abstract

The structure, magnetic and magnetocaloric properties of  $Nd_2Fe_{17-x}Co_x$  ( $x = 0; 1; 2; 3, 4$ ) and  $Gd_2Fe_{17-x}Cu_x$  ( $x = 0, 0.5, 1$  and  $1.5$ ) solid solutions have been studied. For this purpose, these samples were prepared by arc melting and subsequent annealing at 1073 K for a 7 days. Structural analysis by Rietveld method on X-ray diffraction (XRD) have determined that these alloys crystallize in the rhombohedral  $Th_2Zn_{17}$ -type structure (Space group  $R\bar{3} m$ ) and the substitution of iron by nickel and copper leads to a decrease in the unit cell volume. The Curie temperature ( $T_C$ ) of the prepared samples depends on the nickel and copper content. Based on the Arrott plot, these analyses show that  $Nd_2Fe_{17-x}Co_x$  exhibits a second-order ferromagnetic to paramagnetic phase transition around the Curie temperature. These curves were also used to determine the magnetic entropy change  $\Delta S_{Max}$  and the relative cooling power. For an applied field of 1.5 T,  $\Delta S_{Max}$  increase from 3.35 J/kg. K for  $x = 0$  to 5.83 J/kg. K for  $x = 2$ . In addition the RCP increases monotonously. This is due to an important temperature range for the magnetic phase transition, contributing to a large  $\Delta S_{Max}$  shape.  $Gd_2Fe_{17-x}Cu_x$  solid solution has a reduction of the ferromagnetic phase transition temperature from 475 K (for  $x = 0$ ) to 460 K (for  $x = 1.5$ ) is due to the substitution of the magnetic element (Fe) by non-magnetic atoms (Cu). The magnetocaloric effect was determined in the vicinity of the Curie temperature  $T_C$ . By increasing the Cu content, an increase in the values of magnetic entropy ( $\Delta S_{Max}$ ) in a low applied field is observed.

**Keywords:** Rare-earth alloys and compounds, magnetization, magnetocaloric effect

## 1. Introduction

During the last decades and until now, the production of cold has mainly been ensured by the technique of compression/expansion of a refrigerant. This process is developed and reliable, however it has a large number of disadvantages due to the use of toxic gases such as chlorofluorocarbon (CFC) or hydrochlorofluorocarbon (HCFC) which have proved to be very harmful to the environment (destruction of the ozone layers) and contribute to the greenhouse effect. Current environmental requirements and ecological standards limit conventional technologies. It is for this

reason that researchers and manufacturers of refrigeration and heat pump have set out to search for a new refrigeration technology that is more respectful of the environment and less energy intensive, which is magnetic refrigeration (RM).

This cold production technology, which is based on a physical phenomenon called the magnetocaloric effect (EMC), has considerable advantages over conventional techniques: absence of atmospheric pollutants, absence of noise and vibration, high reliability thanks to the use solid refrigerants rather than harmful gases and above all environmental protection and reduction of electricity consumption.

In this regard, in order to get rid of harmful refrigerants, additional efforts have been turned towards the search for magnetocaloric materials. Much attention in this area has been focused on intermetallic compounds which are defined as solid phases containing two or more metals, possibly with one or more non-metallic elements, whose crystal structure differs from that of the constituent elements. In 1997, Pecharsky and Gschneidner reported the discovery of a giant magnetocaloric effect in the intermetallic compounds  $Gd_5(Si_xGe_{1-x})_4$  and  $Gd_5(Si_xGe_2)$  [1–3] which are currently the benchmarks in the field of magnetic refrigeration.

Intermetallic compounds combining rare earths and transition metals have been the subject of much research work in recent years, aiming at their development for technological applications such as magnetic refrigeration, aeronautical turbines [4], battery electrodes [5], and the development of high performance permanent magnets [6] such as the compound  $Nd_2Fe_{14}B$  which has a coercive field equal to 2.3 T [7]. These magnetic materials are now model compounds combining the localized magnetism of rare earth elements and the less localized, or even itinerant, of transition elements.

Long-range magnetic order is mainly found in intermetallic compounds that are based on 4f rare-earth metals (R) and 3d transition metals (M), and in which occur three types of exchange interactions, namely: (1) the 3d–3d exchange interaction (JMM) between the magnetic moments of the M sublattice, (2) the 4f–4f exchange interaction (JRR) between the magnetic moments within the R sublattice, and (3) the intersublattice 3d–4f exchange interaction (JRM). It is noteworthy that the interactions between the rare-earth spins 4f–4f are supposed to be negligible in comparison with the other two types of interactions [8–19].

Recent interest in these  $R_2Fe_{17}$  intermetallic compounds has been renewed due to the magnetocaloric properties shown by these ferromagnetic compounds  $Pr_2Fe_{17}$ ,  $Nd_2Fe_{17}$ ,  $Er_2Fe_{17}$ ,  $Gd_2Fe_{17}$ ,  $Sm_2Fe_{17}$  and  $Tb_2Fe_{17}$  [20–25]. The selected ferromagnetic compound  $Gd_2Fe_{17}$  studied in this research has a magnetocaloric effect with a maximum magnetic entropy  $\Delta S_{Max}$  equal to 0.89 J/kg K, for an external field change from 0 T to 1.5 T at room temperature [24]. The goal here was to study the M effect on structural, and magnetic properties of  $R_2Fe_{17-x}Co_x$ . In our case the Fe and M structure factors are very similar, which makes difficult to localize the M atom in the structure using the X-ray powder diffraction.. Finally, we have studied the low field magnetic entropy changes in  $R_2Fe_{17}$  compounds and we have demonstrated the magnetocaloric effect enhancement due to M substitution, observed for the first time for intermetallic compounds. A systematic study of the constitutional properties of a ternary phase diagram formed by Sm-Fe-Ni and Nd-Fe-Co have been studied by our group [26, 27]. The substitution of Ni or Co by Fe atoms confirmed a extension of binaries  $Nd_2Fe_{17}$  and  $GdFe_{17}$  in the Nd-Fe-Co and Nd-Fe-Co ternary systems, respectively and improved physical support properties and structural stability [28, 29].

## 2. Crystallographic study of the solid solution $R_2Fe_{17-x}M_x$

The  $R_2Fe_{17}$  binaries are generally either of rhombohedral symmetry of type  $Th_2Zn_{17}$  ( $R\bar{3}m$ ) for light rare earths (from Ce to Gd), or of hexagonal symmetry of

type  $\text{Th}_2\text{Ni}_{17}$  ( $\text{P}6_3/\text{mmc}$ ) for heavy rare earths, such as Tb and Dy. These structures derive from the  $\text{CaCu}_5$  structure and differ in the stacking mode of the  $\text{CaCu}_5$  unit entities in **Figures 1** and **2**.

- $\text{Th}_2\text{Zn}_{17}$  has nine entities per cell where three rare earth atoms have each been replaced by an M-M dumbbell (Dumbbell site). This description can be schematized by:

$$9 \text{ RM}_5 - 3 \text{ R} + 3 \times (2\text{M}) = 3 \text{ R}_2\text{M}_{17} \quad (1)$$

- $\text{Th}_2\text{Ni}_{17}$  has six entities per cell where two rare earth atoms have each been replaced by a M-M dumbbell (Dumbbell site). This description can be schematized by:

$$6 \text{ RM}_5 - 2 \text{ R} + 2 \times (2\text{M}) = 2 \text{ R}_2\text{M}_{17} \quad (2)$$

The equilibrium binary compound  $\text{Nd}_2\text{Fe}_{17}$  crystallizes in the  $\text{Th}_2\text{Zn}_{17}$  structure type of space group  $R\bar{3}m$  in **Figure 2** with the lattice parameters  $a = 8.5796$  (3) Å and

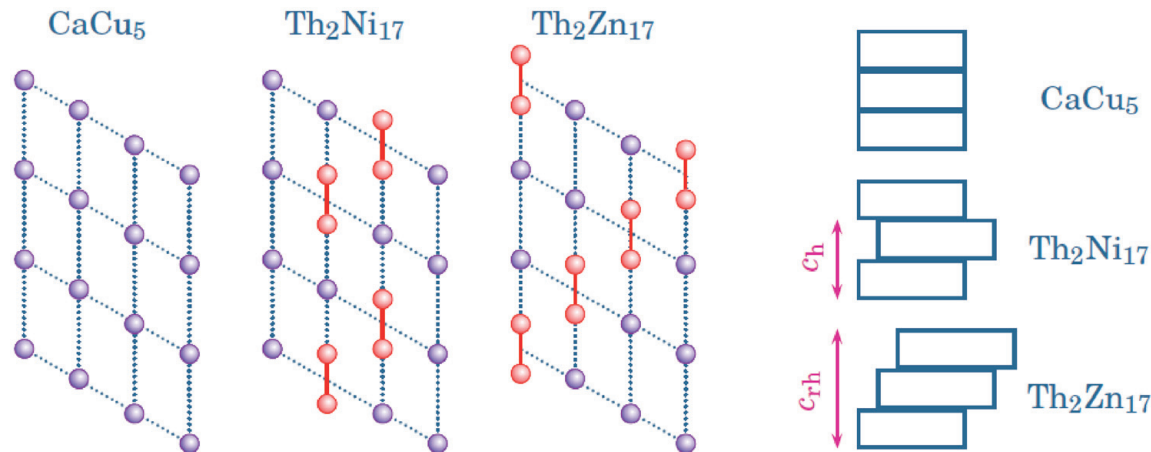


**Figure 1.**  
 2/17 stoichiometric structures derived from  $\text{CaCu}_5$ :  $\text{Th}_2\text{Zn}_{17}$  ( $R\bar{3}m$ ) and  $\text{Th}_2\text{Ni}_{17}$  ( $\text{P}6_3/\text{mmc}$ ).

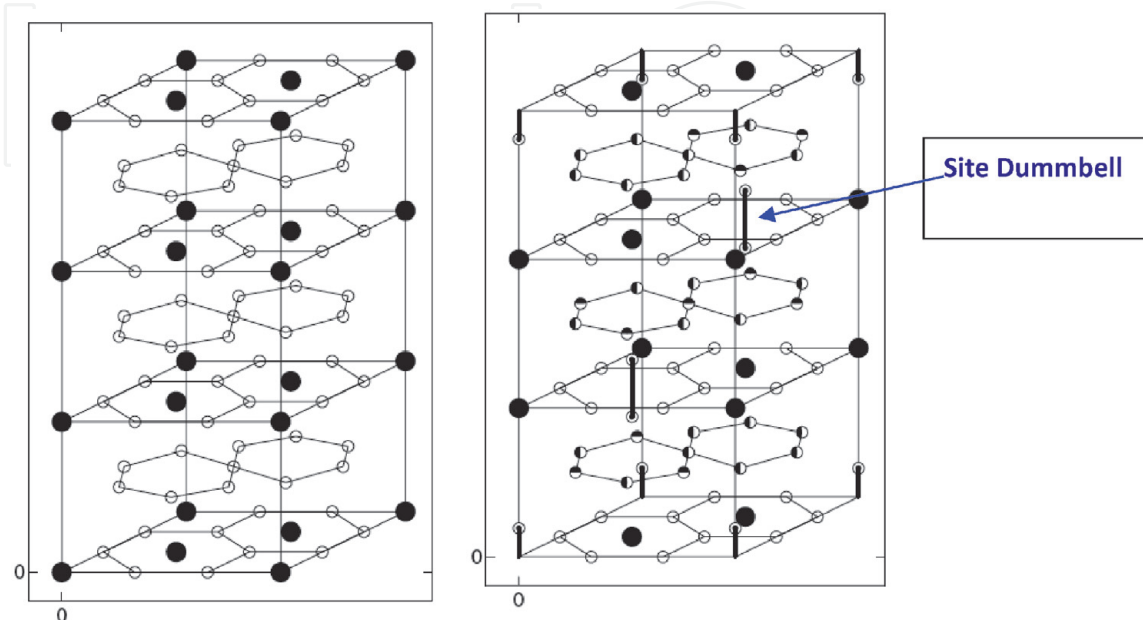


**Figure 2.**  
 Mailles  $P6/mmm$  de type  $\text{CaCu}_5$  (a) et  $R\bar{3}m$  de type  $\text{Th}_2\text{Zn}_{17}$  (b).

$c = 12.4624(2)$  Å. They agree with those found in the literature [30]. This rhombohedral phase  $\bar{R}\bar{3}m$  can be stabilized by certain elements such as Co [31], Cr [32], Si [33] or Ga [34]. The compound  $\text{Sm}_2\text{Fe}_{17}$  as representative of the solid solution crystallizes in a rhombohedral cell of space group  $\bar{R}\bar{3}m$  as was mentioned by X. C. Kou et al. [35]. The atoms of the rare earth occupy the crystallographic sites 6c while the iron atoms occupy 4 unequal sites: 6c, 18 h, 18f and 9d.

The most widely used synthesis method for the production of intermetallic is the melting method, which makes it possible to obtain materials in a solid state followed by annealing or grinding after annealing. Using arc furnace melting followed by annealing for one week, well adequate to ensure good crystallization and complete atomic diffusion. To control the stoichiometry and to avoid impurities, we have optimized the conditions for developing these phases using this method from work published by our laboratory [36, 37]. The development step is followed by a crystallographic study which allowed us to determine the nature of the site occupied by the metal transition and metalloids as well as the crystallographic parameters. This structural study is done by the X-ray diffraction method followed by Rietveld refinement, coupled with studies by scanning electron microscopy.

### 3. Structural of the solid solution $\text{Nd}_2\text{Fe}_{17-x}\text{Co}_x$ ( $0 \leq x \leq 4$ )

The samples synthesized along the  $\text{Nd}_2\text{Fe}_{17-x}\text{Co}_x$  line show the existence of a solid solution which crystallizes in an  $\bar{R}\bar{3}m$  cell of  $\text{Th}_2\text{Zn}_{17}$  type structure extending along the  $0 \leq x \leq 4$  domain.

The lattice parameters and atomic positions determined from the refinement of the few compositions synthesized on the line of the binary extension  $\text{Nd}_2\text{Fe}_{17-x}\text{Co}_x$  ( $0 \leq x \leq 4$ ) are grouped together in **Tables 1** and **2**.

The Rietveld refinements of the  $\text{Nd}_2\text{Fe}_{17-x}\text{Co}_x$  series ( $0 \leq x \leq 4$ ) are shown in **Figure 3**.

| Compositions | $a$ (Å)   | $c$ (Å)    | $c/a$ | $\chi^2$ | $R_B$ |
|--------------|-----------|------------|-------|----------|-------|
| $x = 0$      | 8.5792(2) | 12.4615(2) | 1.452 | 1.97     | 7.18  |
| $x = 1$      | 8.5763(2) | 12.4606(3) | 1.452 | 3.57     | 6.78  |
| $x = 2$      | 8.5597(2) | 12.5069(4) | 1.461 | 2.47     | 3.3   |
| $x = 3$      | 8.5594(3) | 12.5081(4) | 1.463 | 2.77     | 3.3   |
| $x = 4$      | 8.5598(3) | 12.5069(4) | 1.461 | 2.47     | 7.51  |

**Table 1.**  
The lattice parameters of the  $\text{Nd}_2\text{Fe}_{17-x}\text{Co}_x$  system ( $0 \leq x \leq 4$ ).

| Atomes | Positions de Wyckoff | $x$     | $y$     | $z$     | Occupation |
|--------|----------------------|---------|---------|---------|------------|
| Nd     | 6c                   | 0.00000 | 0.00000 | 0.34304 | 1          |
| Fe1    | 18f                  | 0.29276 | 0.00000 | 0.00000 | 1          |
| Fe2    | 9d                   | 0.50000 | 0.00000 | 0.50000 | 1          |
| Fe3    | 6c                   | 0.00000 | 0.00000 | 0.09938 | 1          |
| Fe4    | 18 h                 | 0,5     | 0,5     | 0.15679 | 0,334      |
| Co4    | 18 h                 | 0,5     | 0,5     | 0.15679 | 0,666      |

**Table 2.**  
Atomic positions ( $x, y, z$ ) and occupation of the various Wyckoff positions for the compound  $\text{Nd}_2\text{Fe}_{13}\text{Co}_4$ .

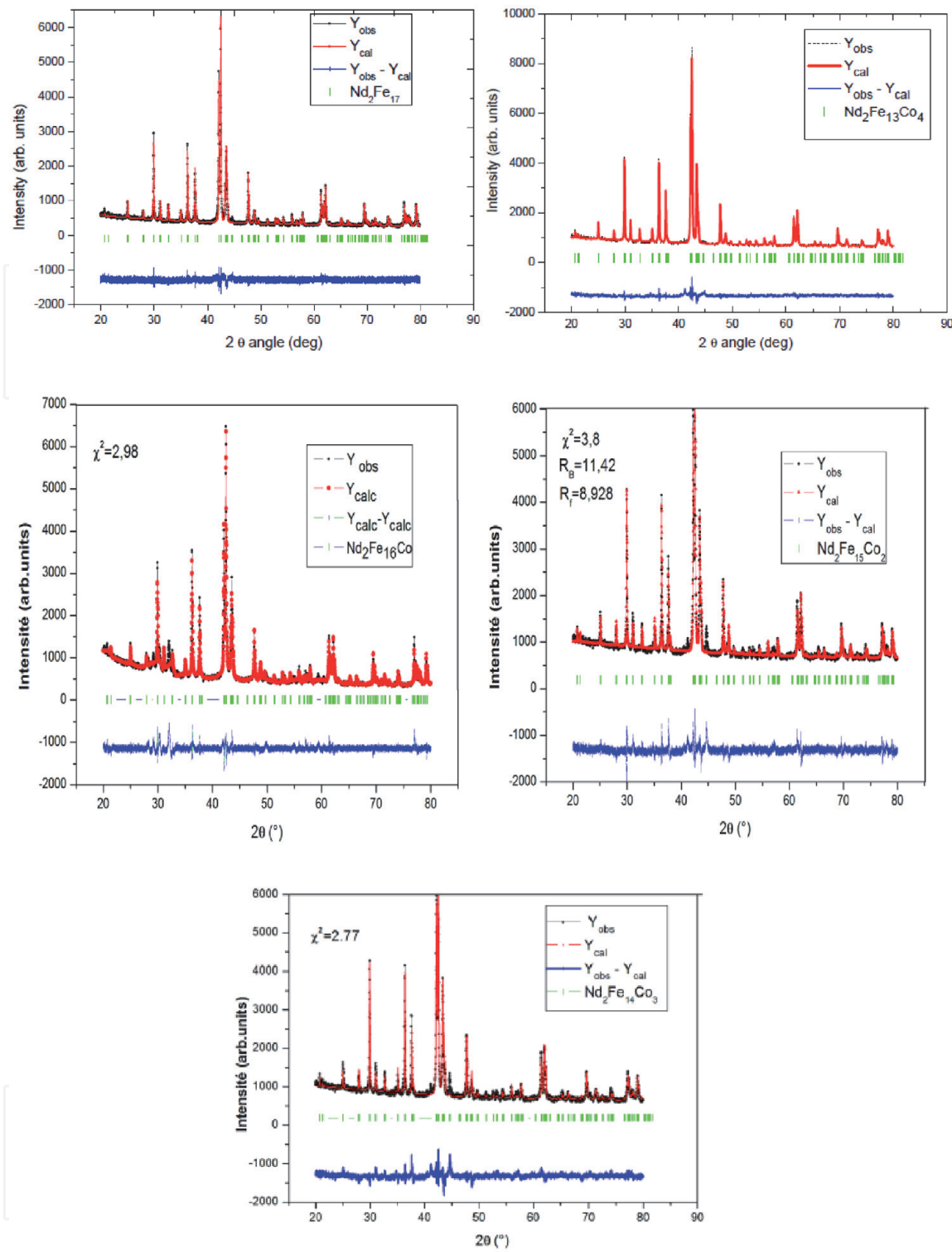


**Figure 3.**  
 Rietveld refinements results of the solid solution  $Nd_2Fe_{17-x}Co_x$  ( $0 \leq x \leq 4$ ).

The unit cell parameters for  $Nd_2Fe_{17}$  obtained are:  $a = 8.5792(2)$  Å,  $c = 12.4615(2)$  Å, and  $a = 8.5598(3)$  Å,  $c = 8.5598(3)$  Å, for  $Nd_2Fe_{17}$  and  $Nd_2Fe_{13}Co_4$  compounds, respectively.

The effect of Co on the lattice parameter is quite weak up to  $x = 4$ , the parameter  $a$  shows a tendency to decrease,  $\Delta a / a \approx -5.6 \times 10^{-4}$  per atom of cobalt, on the other hand the parameter  $c$  increases slightly  $\Delta c / c = 9.3 \times 10^{-4}$  per atom of cobalt, but the volume and the  $c/a$  ratio remains almost constant (**Figure 4**). While  $c/a$  is almost constant. The atomic positions are not affected by the substitution.

Our results are in agreement with those of Li et al. [38]. For these authors  $c$  increases until  $x = 2$  whereas we have measured without any ambiguity a slight

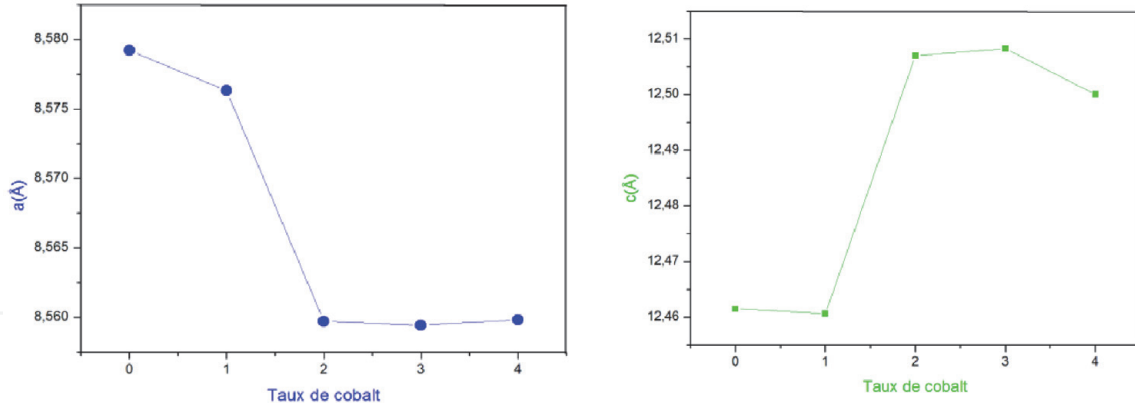


**Figure 4.**  
Variation of parameters  $a$  and  $c$  for  $Nd_2Fe_{17-x}Co_x$ , as a function of the level of cobalt  $x$ .

increase. On the other hand, our results are in agreement with the decrease found by Lin et al. [39]. Atomic positions are not affected by substitution. A. Nandra et al. [40], obtained the converse. There is also a decrease in  $c$ , equal to  $6.5 \times 10^{-3}$  Å per small silicon atom compared to the variation in an equal to  $19 \times 10^{-3}$  Å per silicon atom. Moreover, the parameter values found for  $Sm_2Fe_{15}Si_2$  and  $Sm_2Fe_{16}Si$  [41, 42], confirm these results. In general, the evolution of lattice parameters, in solid solutions  $R_2Fe_{17-x}Si_x$ , depends on the nature of the rare earth R. For  $R = Ce$ ,  $a$  decreases while  $c$  increases, for  $R = Dy, Y$  both parameters decrease [43, 44]. A simple steric effect of substitution of iron with radius  $r_{Fe} = 1.274$  Å by a smaller atom can nevertheless explain such an evolution if we consider the covalent radius of cobalt equal to 1.252 Å.

#### 4. Structural of the solid solution: $Gd_2Fe_{17-x}Cu_x$ $0 \leq x \leq 1.5$

Scanning electron microscopy analyzes coupled with X-ray diffractograms identified using PowderCell software reveal a solubility domain of  $Gd_2Fe_{17-x}Cu_x$  that extends up to  $x = 1.5$ . Whereas, the solubilities of Ti, Mo and Re in the binary  $Gd_2Fe_{17}$  [39–41] are of order 2.3; 0.06 and 1.5 at%, respectively. The X-ray powder diffraction diagram (Figure 5) of the nominal composition  $Gd_6-Fe_{14}-Cu_9$  is

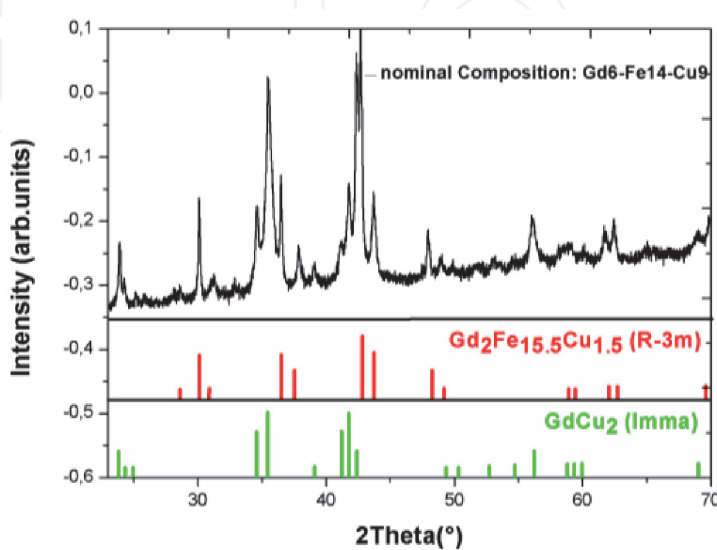


**Figure 5.**  
X-ray diffractogram of the alloy of nominal composition  $Gd_6-Fe_{14}-Cu_9$  located in binary region 4 showing the bi-phasic equilibrium between:  $GdCu_2 + Gd_2Fe_{15.5}Cu_{1.5}$ .

indexed on the basis of the two rhombohedral and orthorhombic cells indicating the equilibrium thermodynamics between the compound  $\text{GdCu}_2$  and the limit of the solid solution  $\text{Gd}_2\text{Fe}_{17-x}\text{Cu}_x$  with  $x = 1.5$  [45–47].

The SEM image reconstituted from backscattered electrons of the compound  $\text{Gd}_6\text{Fe}_{14}\text{Cu}_9$  annealed at 800° C (**Figure 6**) is in good agreement with the result found by the X-ray powder diffraction, since we see there two main types of contrasts which correspond to each of the two phases  $\text{GdCu}_2$  and  $\text{Gd}_2\text{Fe}_{15.5}\text{Cu}_{1.5}$ .

To show the extension of the binary  $\text{Gd}_2\text{Fe}_{17}$  in the ternary system, and to make a study of the structural, we synthesized three single-phase samples along the line  $\text{Gd}_2\text{Fe}_{17-x}\text{Cu}_x$  ( $x = 0.5; 1$  and  $1.5$ ). **Figure 7** shows the Rietveld refinement of the X-ray diffractograms of those compounds which crystallize in the rhombohedral structure with the  $\bar{R}-\bar{3}m$  space group. These diffractograms show no structural phase transition following the substitution of iron by copper.

We have demonstrated the formation of a new solid solution  $\text{Gd}_2\text{Fe}_{17-x}\text{Cu}_x$  ( $0 \leq x \leq 1.5$ ). Following the Rietveld refinement, it was concluded that the limit of

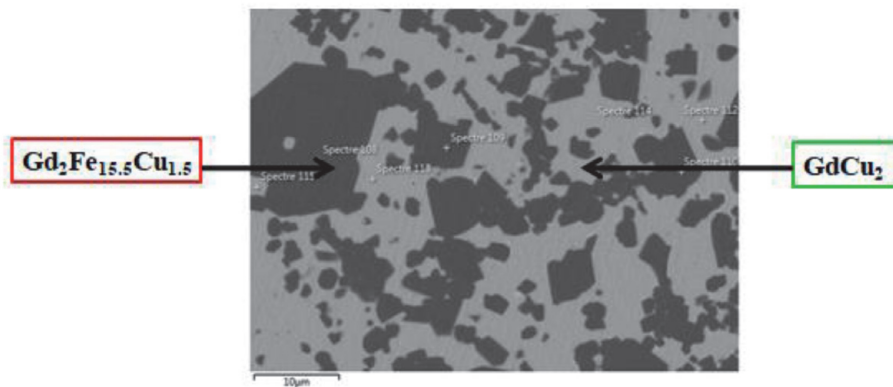


**Figure 6.**  
 SEM-EDS image of the alloy of nominal composition  $\text{Gd}_6\text{Fe}_{14}\text{Cu}_9$  showing the limit of solid solution  $\text{Gd}_2\text{Fe}_{17-x}\text{Cu}_x$  and the three-phase equilibrium between  $\text{GdCu}_2$  and  $\text{Gd}_2\text{Fe}_{15.5}\text{Cu}_{1.5}$ .

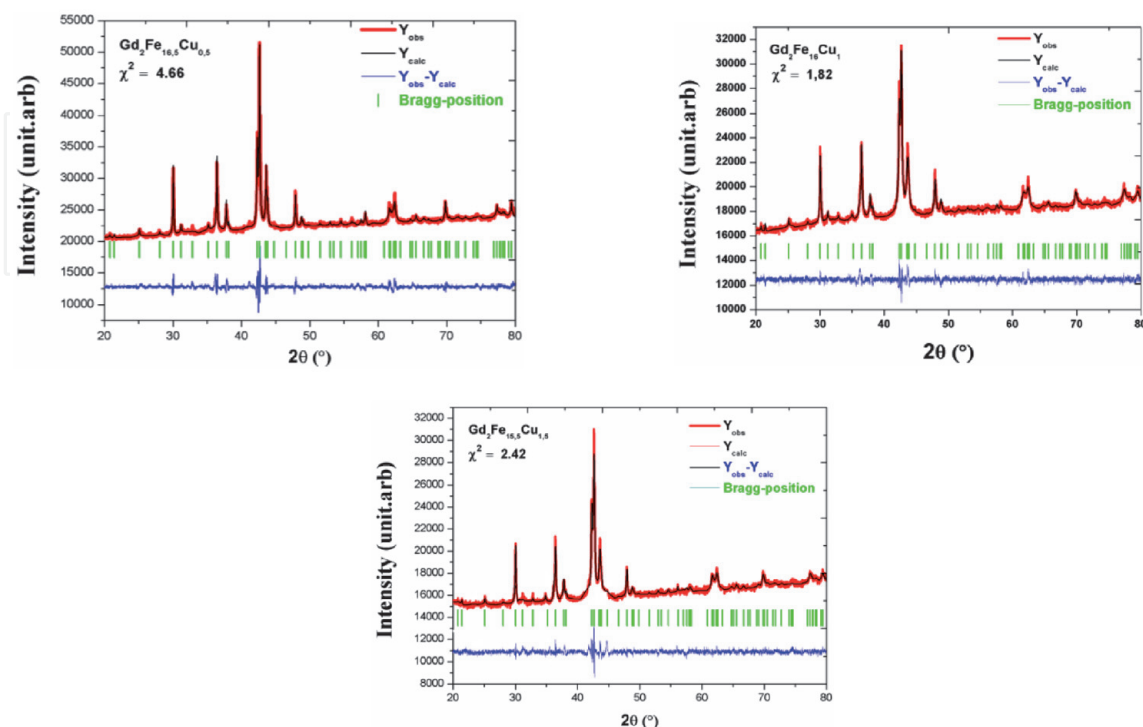


**Figure 7.**  
 Refinement of the samples of the solid solution  $\text{Gd}_2\text{Fe}_{17-x}\text{Cu}_x$  ( $x = 0.5; 1; 1.5$ ).

the solid solution  $\text{Gd}_2\text{Fe}_{17-x}\text{Cu}_x$  corresponds to  $\text{Gd}_2\text{Fe}_{15.5}\text{Cu}_{1.5}$ . The results of structural analyzes obtained by the Rietveld refinement of X-ray diffraction data are referenced in **Table 3**.

The Rietveld refinements of X-ray diffraction diagrams made it possible to follow the evolution of lattice parameters as a function of the copper content. The decrease in the lattice parameters  $a$  and  $c$  in these compounds following the substitution of iron by copper can be explained in terms of the atomic size of the element substituted for Fe. We also notice that the lattice volume of the  $\text{Gd}_2\text{Fe}_{17-x}\text{Cu}_x$  system decreases by increasing the Cu level.

The Rietveld refinement of the compounds of the solid solution  $\text{Gd}_2\text{Fe}_{17-x}\text{Cu}_x$  was carried out according to the standard procedure. For an occupation of copper at site 6c, 9d, 18 h or 18f, the lattice parameters, atomic positions and line profile parameters were considered as adjustable parameters. The best agreement is found for a copper substitution at the 18 h site. From this result, we concluded that copper only substitutes at the 18 h site. However, the Rietveld refinement of  $\text{Gd}_2\text{Fe}_{17-x}\text{Ti}_x$  studied by G. Pokharel et al. [48] proves that the substitution of titanium by iron was made in the two sites 18 h and 18 f. For the solid solution  $\text{Gd}_2\text{Fe}_{17-x}\text{Si}_x$ , the preferred silicon substitution site is 18 h [49].

**Figure 8** shows the rhombohedral crystal lattice of the compound  $\text{Gd}_2\text{Fe}_{16.5}\text{Cu}_{0.5}$ . The gadolinium atoms occupy the crystallographic site (6c) with an occupancy rate equal to 1 and the atoms Fe1, Fe2, and Fe3 are located respectively in the three unequal sites 6c, 9d, 18f with an occupancy rate of order 1. The two atoms

| Composition                                  | Groupe d'espace   | $a$ (Å)  | $c$ (Å)   | $V$ (Å <sup>3</sup> ) | $\chi^2$ | $R_B$ | $R_F$ |
|--|-------------------|----------|-----------|-----------------------|----------|-------|-------|
| $\text{Gd}_2\text{Fe}_{16.5}\text{Cu}_{0.5}$ | $\bar{R}\bar{3}m$ | 8,539(6) | 12,436(7) | 785,554(5)            | 4,66     | 5,37  | 5,10  |
| $\text{Gd}_2\text{Fe}_{16}\text{Cu}_1$       | $\bar{R}\bar{3}m$ | 8,534(4) | 12,433(3) | 784,254(2)            | 1,82     | 3,54  | 3,57  |
| $\text{Gd}_2\text{Fe}_{15.5}\text{Cu}_{1.5}$ | $\bar{R}\bar{3}m$ | 8,533(5) | 12,426(6) | 783,748(4)            | 2,42     | 11,2  | 15,3  |

**Table 3.**  
Crystallographic parameters of the solid solution  $\text{Gd}_2\text{Fe}_{17-x}\text{Cu}_x$  ( $x = 0.5$ ; 1 and 1.5).

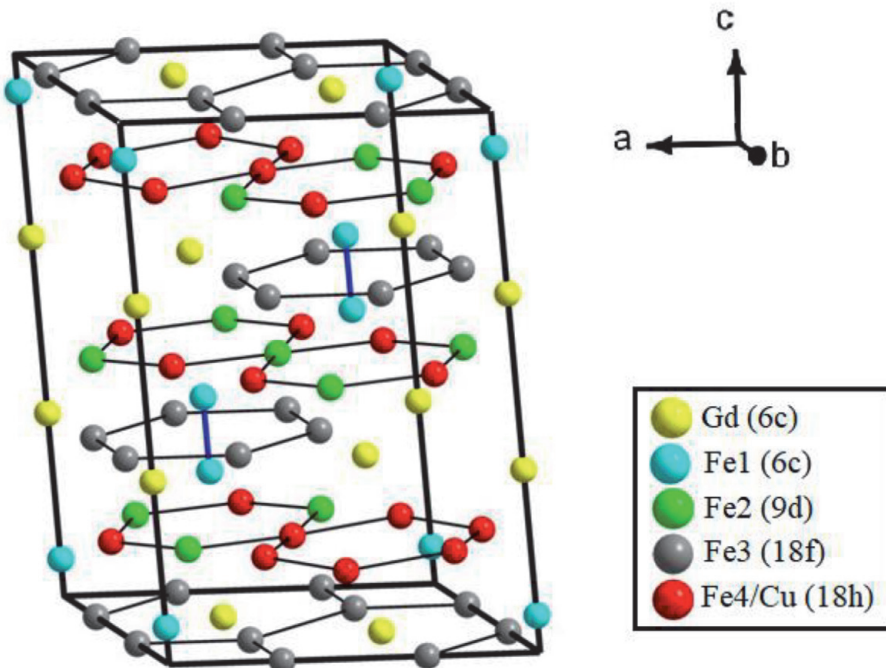


**Figure 8.**  
Schematic representation of a rhombohedral  $\bar{R}\bar{3}m$  crystal structure of  $\text{Gd}_2\text{Fe}_{16.5}\text{Cu}_{0.5}$ .

| Atomes | Sites de Wyckoff | Position des sites |       |       | Occupation |
|--------|------------------|--------------------|-------|-------|------------|
|        |                  | X                  | Y     | Z     |            |
| Gd     | 6c               | 0                  | 0     | 0,336 | 1          |
| Fe1    | 6c               | 0                  | 0     | 0,075 | 1          |
| Fe2    | 9d               | 1/2                | 0     | 1/2   | 1          |
| Fe3    | 18f              | 0,303              | 0     | 0     | 1          |
| Fe4    | 18 h             | 0,501              | 0,499 | 0,160 | 0,916      |
| Cu     | 18 h             | 0,501              | 0,499 | 0,160 | 0,084      |

**Table 4.**  
 Characterization of the atomic sites of the compound  $Gd_2Fe_{16.5}Cu_{0.5}$ .

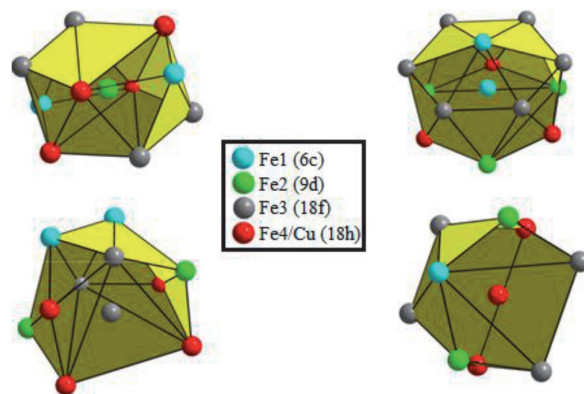


**Figure 9.**  
 The coordination polyhedra for each crystallographic Fe site.

Fe4 and Cu are distributed over the same Wyckoff site (18 h) with an occupancy rate equal to 0.916 and 0.084 respectively. The atomic positions for the different crystallographic sites of the  $R\bar{3}m$  structure are reported in **Table 4**.

In this type of structure we notice the presence of layers formed by hexagons. The hexagons made up of Fe3 atoms (18f) contain gadolinium atoms at the centers. While the hexagons formed by the Fe2 atoms located in the sites (9d) and the Fe4/Cu atoms located in the sites (18 h) are empty.

**Figure 9** shows the coordination polyhedra of the four sites: 6c, 9d, 18f and 18 h. The polyhedron of the Fe2 atom located in site (9d) is an icosahedron consisting of four atoms of Fe4 / Cu (18 h), four atoms of Fe3 (18f) and two atoms of Fe1 (6c). In addition, the Fe1 atom located in site (6c) is surrounded by six Fe3 atoms (18f), three Fe4 / Cu atoms (18 h), three Fe2 atoms (9d) and a single Fe1 atom (6c). Also, the Fe3 atom located in site (18f) is coordinated by two Fe2 atoms (9d), two Fe3 atoms (18f), four Fe4 / Cu atoms (18 h) and two Fe1 atoms (6c) thus forming an icosahedron. Finally, the polyhedron of the Fe3 atom located in site (18 h) is made up of two atoms of Fe2 (9d), four atoms of Fe3 (18f), a single atom of Fe1 (6c) and two atoms of Fe4/Cu (18 h).

## 5. Magnetic and magnetocaloric properties of the solid solution $R_2Fe_{17-x}M_x$

The Curie temperature is the temperature of the transition from the ordered magnetic state (ferromagnetic) to the disordered state (paramagnetic).

This transition is manifested by a sharp drop in magnetic susceptibility measured as a function of temperature.

Remember that in R-Fe intermetallics, the order temperature is determined by the interactions between iron atoms. The nature of these interactions depends on the degree of filling of the 3d band of iron and the Fe-Fe distances. Interatomic distances of less than 2.45 Å promote antiferromagnetic interactions [50]. The  $\text{Sm}_2\text{Fe}_{17}$  compound is characterized by a low Curie temperature [51]. This is mainly due to the short inter-atomic Fe-Fe distances of 6c-6c dumbbells and as well as 9d-18f distances, the corresponding distances being 2.39 Å and 2.44 Å respectively. These distances, less than 2.45 Å, lead to negative Fe-Fe interactions, because these atoms are anti-ferromagnetically coupled [52].

In general, in rare earth intermetallic compounds, the Curie temperature is given by three types of exchange interactions:

- The 3d-3d ( $J_{\text{Fe-Fe}}$ ) exchange between the magnetic moments of the sub-network of iron atoms.
- The 4f -4f exchange ( $J_{\text{R-R}}$ ) between the magnetic moments of rare earth atoms.
- The 3d -4f ( $J_{\text{R-Fe}}$ ) exchange between the two 3d-4f subnets.

Of these three types of exchange interactions, the 4f -4f exchange is the weakest and can be overlooked. However, if we consider an R-Fe system where R is non-magnetic, we can also neglect the interactions between the two sub-networks (3d-4f) and we can consider that the only contribution to the Curie temperature is due to the interaction between the magnetic moments of the iron sub-lattice (3d-3d).

The crystal structure dictates the mode of interaction as well as the intensity of the interaction. These interactions seem to originate from the electronic coupling between close neighboring atoms. The intensity of these interactions is a factor in the distance between carriers. The curve in **Figure 10** shows the exchange

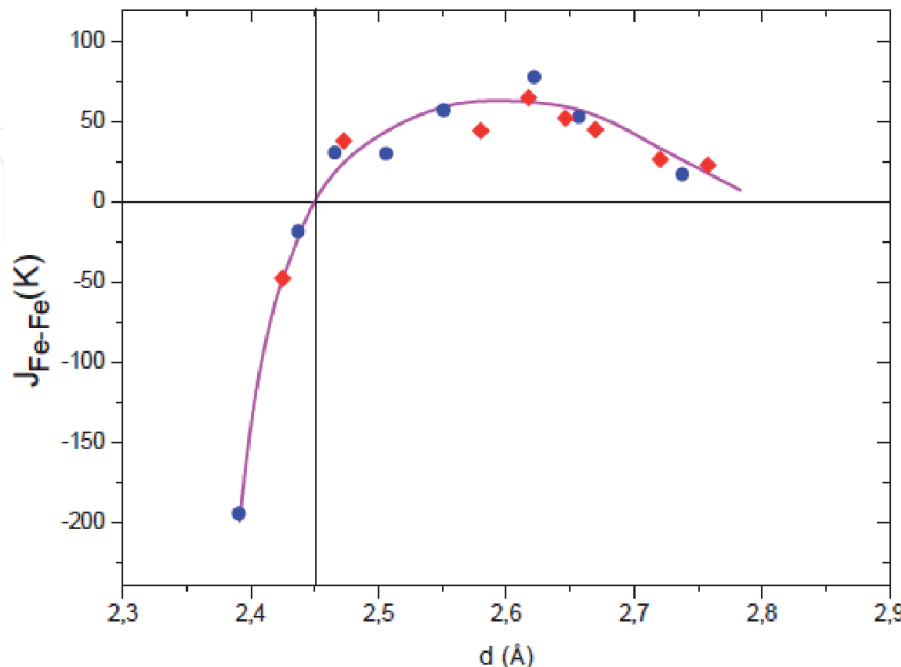


**Figure 10.**  
Exchange interaction as a function of iron–iron distances for the  $\text{Sm}_2\text{Fe}_{17}$  compounds (in lozange) and their nitrides (in circle).

interaction as a function of iron–iron distances for the  $(\text{Gd}, \text{Nd})_2\text{Fe}_{17}$  compounds and their nitrides. The signs and intensity of this integral are closely related to the distance between Fe–Fe for both phase 2/17 and its nitride. Indeed for interatomic distances less than 2.45 Å leads to negative Fe–Fe interactions where the atoms are coupled antiferromagnetically. Beyond that, these interactions become positive, which corresponds to a ferromagnetic coupling between close neighboring iron. The exchange interaction is very intense, but only acts between nearby moments and subsides very quickly with distance. The Curie temperature is the result of two effects: a magnetovolumic effect [53, 54] linked to Fe–Fe distances and an electronic effect linked to the filling of the 3d band of iron.

In order to obtain as much information as possible on the magnetocaloric effect in our intermetallics in the vicinity of their Curie temperature. The variation of the magnetic entropy  $\Delta S_{\text{Max}}$  is evaluated by an indirect method whose main ingredient is magnetic measurement; this method is therefore based on magnetization isotherms as a function of the magnetic field applied for different temperatures. This amounts, for each temperature, to calculating the area between the two isotherms around the temperature of  $T_c$  using the following equations:

$$\Delta S_M(T, \mu_0 H) = S_M(T, \mu_0 H) - S_M(T, 0) = \int_0^{\mu_0 H_{\text{max}}} \left( \frac{\partial S}{\partial (\mu_0 H)} \right) d(\mu_0 H) \quad (3)$$

From Maxwell's thermodynamic relation:

$$\left( \frac{\partial S}{\partial (\mu_0 H)} \right)_T = \left( \frac{\partial M}{\partial T} \right)_{\mu_0 H} \quad (4)$$

We can get the equation:

$$\Delta S_M(T, \mu_0 H) = S_M(T, \mu_0 H) - S_M(T, 0) = \int_0^{\mu_0 H_{\text{max}}} \left( \frac{\partial M}{\partial T} \right)_{\mu_0 H} d(\mu_0 H) \quad (5)$$

Finally, the magnetic entropy was calculated, using software, by the expression:

$$\Delta S_M \left( \frac{T_1 - T_2}{2} \right) = \left( \frac{1}{T_1 - T_2} \right) \left[ \int_0^{\mu_0 H_{\text{max}}} M(T_2, \mu_0 H) d(\mu_0 H) - \int_0^{\mu_0 H_{\text{max}}} M(T_1, \mu_0 H) d(\mu_0 H) \right] \quad (6)$$

## 6. Magnetic and magnetocaloric properties of the solid solution $\text{Nd}_2\text{Fe}_{17-x}\text{Co}_x$

### 6.1 Magnetic properties

Magnetic study of the binary compound  $\text{Nd}_2\text{Fe}_{17}$  reveals the existence of a Curie temperature of the order of  $T_C = 326$  K. These samples show a ferro-paramagnetic type transition. The Curie  $T_C$  temperature was determined from the curves  $(dM/dT)$ . This temperature increases as the concentration of cobalt increases while indicating an increase in ferromagnetism from **Figure 11**. Indeed, Co plays a main role in strengthening 3d-3d interactions. Based on the very short interatomic distances, the low Curie temperature of the  $\text{Nd}_2\text{Fe}_{17}$  compound is due to the level of the Fe–Fe dumbbell pairs, located at the 6c site where the iron atoms are antiferromagnetically coupled.

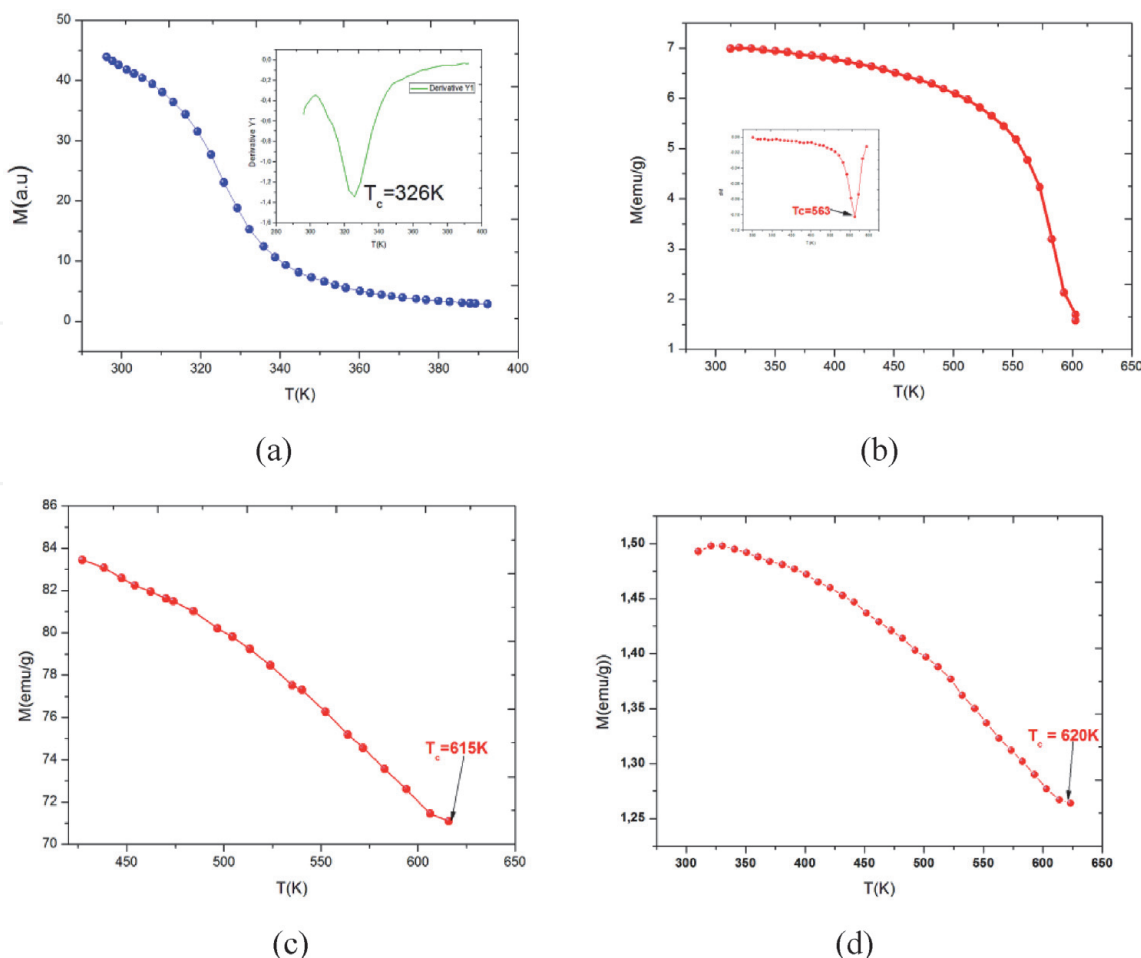


**Figure 11.**  
Magnetization as a function of temperature  $M(T)$  for  $Nd_2Fe_{17}$  (a)  $Nd_2Fe_{15}Co_2$  (b)  $Nd_2Fe_{14}Co_3$  (c)  $Nd_2Fe_{15}Co_4$  (d).

The increase in Curie temperature with the level of cobalt can be attributed, in part, to a reduction in the number of Fe-Fe pairs, coupled antiferromagnetically. Substitution by cobalt induces filling of the 3d band of iron, which promotes positive 3d-3d interactions [55]. In addition, the effect of cobalt is to slightly shift 3d states to higher energies. This more pronounced effect in the minority spin band leads to an increase in iron moment and is partially responsible for the increase in Curie temperature.

## 6.2 Magnetocaloric effect

The variation of the magnetic entropy  $\Delta S_{\text{Max}}$  is evaluated by an indirect method whose main objective is the magnetic measurement; this method is based on isotherms magnetization depending on the magnetic field applied for different temperatures. Indeed, for each temperature, we calculate the area between the two isotherms around the temperature chosen in a range of field divided by the temperature difference between these two curves.

The calculated  $\Delta S$  value for each applied field was calculated from the curves of the isotherm  $M(H)$  (**Figure 12**) using the following equations (Maxwell's relation) Eqs. (1)–(4):

Dans le but de connaître la nature de la transition ferro-paramagnétique, nous avons porté sur la **Figure 13** les isothermes d'Arrott [56] donnant  $M^2$  en fonction de  $H/M$  pour les différentes températures pour toute la gamme de composition x en cobalt.

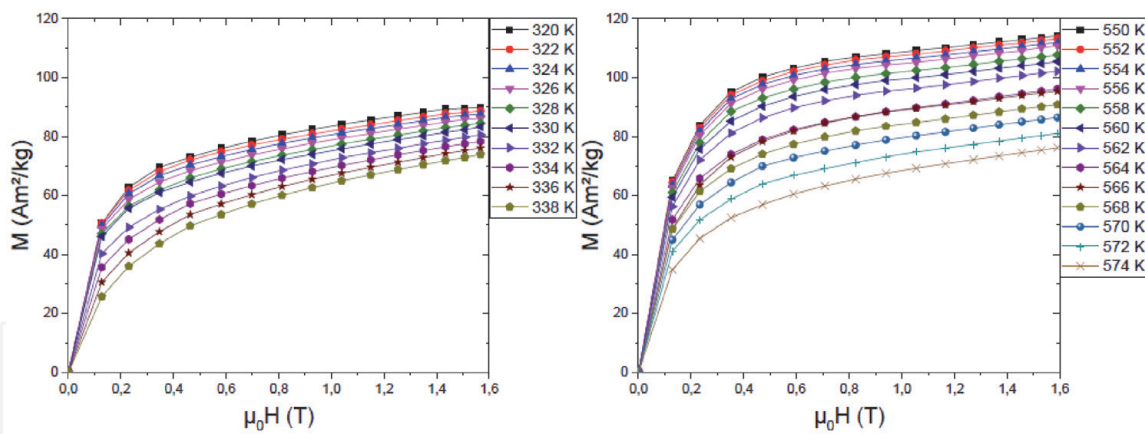


**Figure 12.**  
 Variation of the magnetization as a function of the magnetic field applied for the compounds of  $\text{Nd}_2\text{Fe}_{17}$  (left) and  $\text{Nd}_2\text{Fe}_{15}\text{Co}_2$  (right).

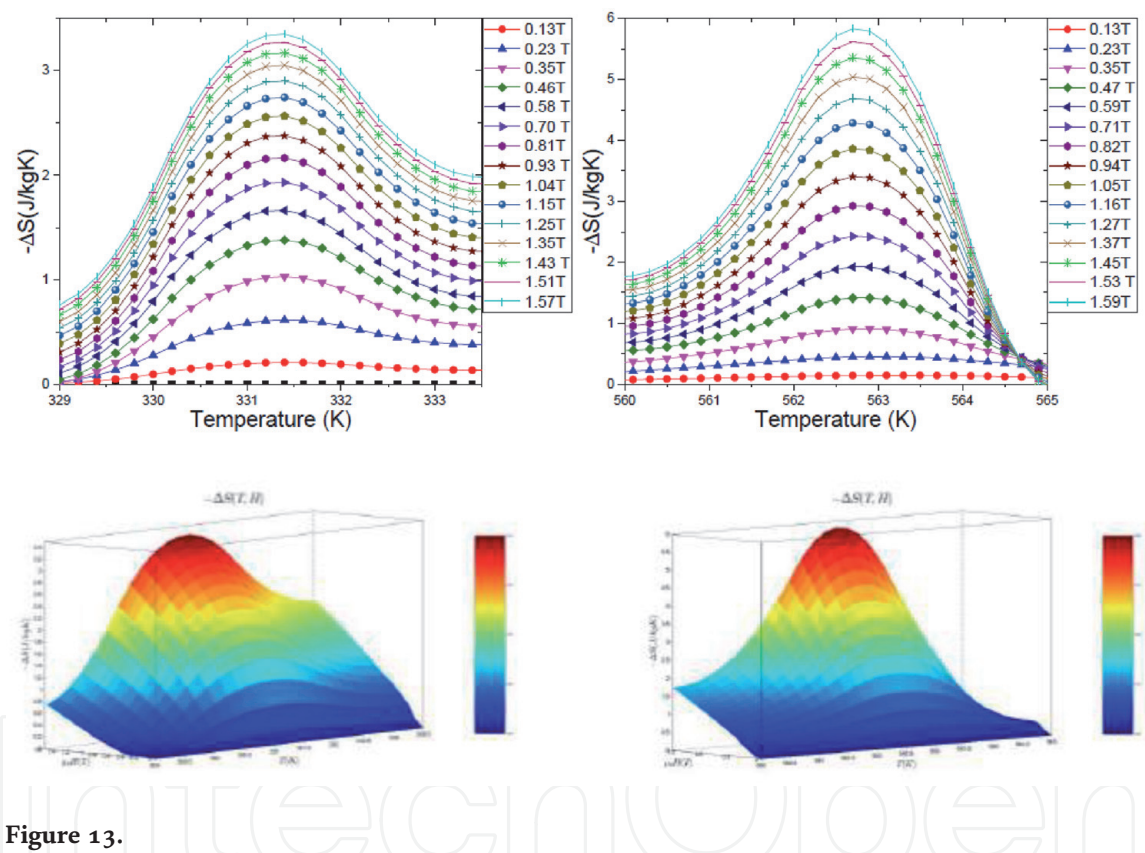


**Figure 13.**  
 Variation of magnetic entropy  $-\Delta S$  ( $T$ ) depending on the temperature and the magnetic field of  $\text{Nd}_2\text{Fe}_{17}$  (left) and  $\text{Nd}_2\text{Fe}_{15}\text{Co}_2$  (right).

The  $\text{Nd}_2\text{Fe}_{17-x}\text{Co}_x$  magnetocaloric properties were determined and calculated from the magnetization measured as a function of the magnetic field at different constant temperatures. In order to continue the study of the effect of cobalt on the magnetic and magnetocaloric properties of our compound, we studied the change of entropy  $-\Delta S$  ( $T$ ). The variation of the magnetic entropy  $\Delta S$  is evaluated by an indirect method whose the main objective is magnetic measurement, this method is based on magnetization isotherms as a function of the magnetic field applied for different temperatures. Indeed, for each temperature, we calculate the area between the two isotherms around the temperature chosen in a range of field divided by the temperature difference between these two curves.

For magnetocaloric applications, it is interesting to determine the relative refrigeration capacity (which we will note RCP or relative cooling power). It is the

| x                              | 0    | 2    |
|--------------------------------|------|------|
| T <sub>c</sub>                 | 331  | 563  |
| (-ΔS <sub>Max</sub> ) (J/kg.K) | 3.35 | 5.83 |
| RCP(J/kg)                      | 11.6 | 16   |

**Table 5.**

Summary of magnetocaloric properties of  $Nd_2Fe_{17-x}Co_x$  system ( $x = 0$  and  $x = 2$ ).

amount of heat that can be transferred from the hot source to the cold source in a refrigerator. This parameter is related to the variation of magnetic entropy according to the following relationship [57]:

$$RCP = -\Delta S_{Max} \times \delta T_{FWHM}$$

**Table 5** shows that the values of the maximum magnetic entropy and the cooling capacity (RCP) of the compounds in the solid solution  $Nd_2Fe_{17-x}Co_x$  ( $x = 0$  and  $x = 2$ ) increase with the copper content.

Indeed, the values of the magnetic entropy of the  $Nd_2Fe_{17-x}Co_x$  system are close to those determined in the  $R_2Fe_{17}$  system ( $R$ : Gd, Tb, Dy and Er) [58], as well as in solid solutions  $Pr_2(Fe, Al)_{17}$  and  $(Pr, Dy)_2Fe_{17}$  [59].

## 7. Magnetic and magnetocaloric properties of the solid solution $Gd_2Fe_{17-x}Cu_x$

### 7.1 Magnetic properties of the $Gd_2Fe_{17-x}Cu_x$ series ( $0 \leq x \leq 1.5$ )

Magnetic measurements of the temperature dependence of the magnetization were performed using a DSM-8 Differential Magneto /Susceptometer, in the temperature range from 300 K up to 600 K and under a weak applied magnetic field of order 0.12 T. From the M (T) curves of the series of compounds  $Gd_2Fe_{17-x}Cu_x$  ( $x = 0; 0.5; 1$  and  $1.5$ ) shown in **Figure 14**.

The study of the evolution of the magnetization as a function of the temperature and of the M (H, T) field carried out on either side of the Curie temperature with a step of 5 K for each compound of the solid solution  $Gd_2Fe_{17-x}Cu_x$  ( $x = 0; 0.5; 1$  and  $1.5$ ). These magnetization isotherms clearly show that our samples exhibit paramagnetic behavior for high temperatures and ferromagnetic behavior for temperatures below the  $T_C$ . At low temperatures ( $T < T_C$ ), the curves show a rapid increase in magnetization for a field  $H < 1$  T and as soon as the applied magnetic field increases, the magnetization tends to saturate. We note that with a field of the order of 1 T, the studied compounds reach saturation. For ( $T > T_C$ ), the magnetization curves as a function of the magnetic field applied at different temperatures become more and more linear. **Figure 15** shows the isothermal magnetization curves measured under a magnetic field variation of 0–2 T, of the compounds of the solid solution  $Gd_2Fe_{17-x}Cu_x$  ( $x = 0; 0.5; 1$  and  $1.5$ ).

The Arrott method allows us to study the order of the magnetic transition of  $Gd_2Fe_{17-x}Cu_x$  samples ( $0 \leq x \leq 1.5$ ) using the isotherms M (H, T). For a second-order transition, the Arrott curves have positive slopes while for a first-order transition, the curves are negative. The Arrott isotherms presented in **Figure 16** for the  $Gd_2Fe_{17-x}Cu_x$  samples ( $x = 0; 0.5; 1$  and  $1.5$ ) show positive slopes which reveals the presence of a second order magnetic transition for all the samples.

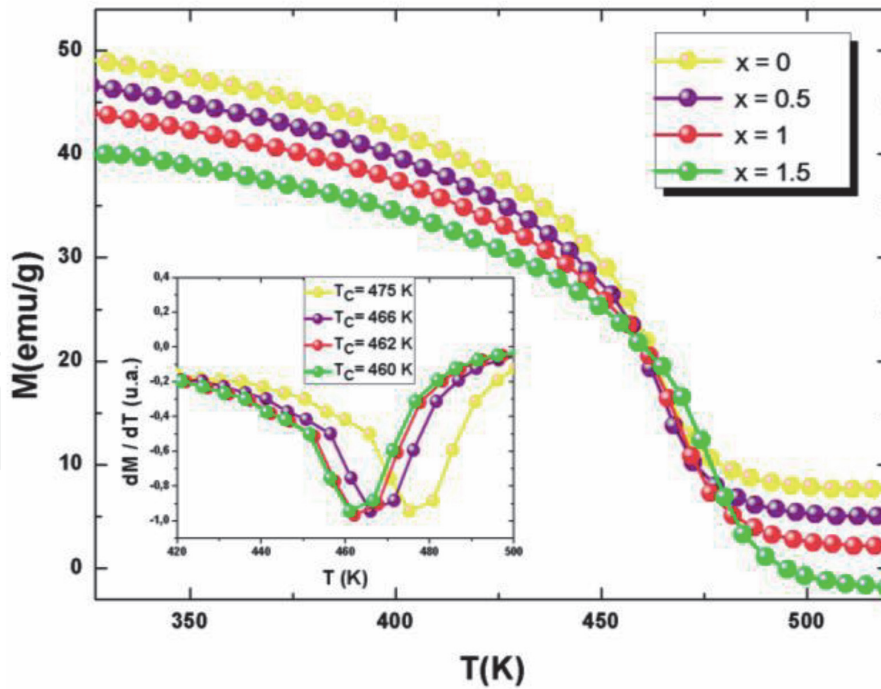


**Figure 14.**  
*Evolution of the magnetization as a function of the temperature  $M$  ( $T$ ) for  $Gd_2Fe_{17-x}Cu_x$  ( $x = 0; 0.5; 1$  and  $1.5$ ) under a field of  $0.12$  T.*

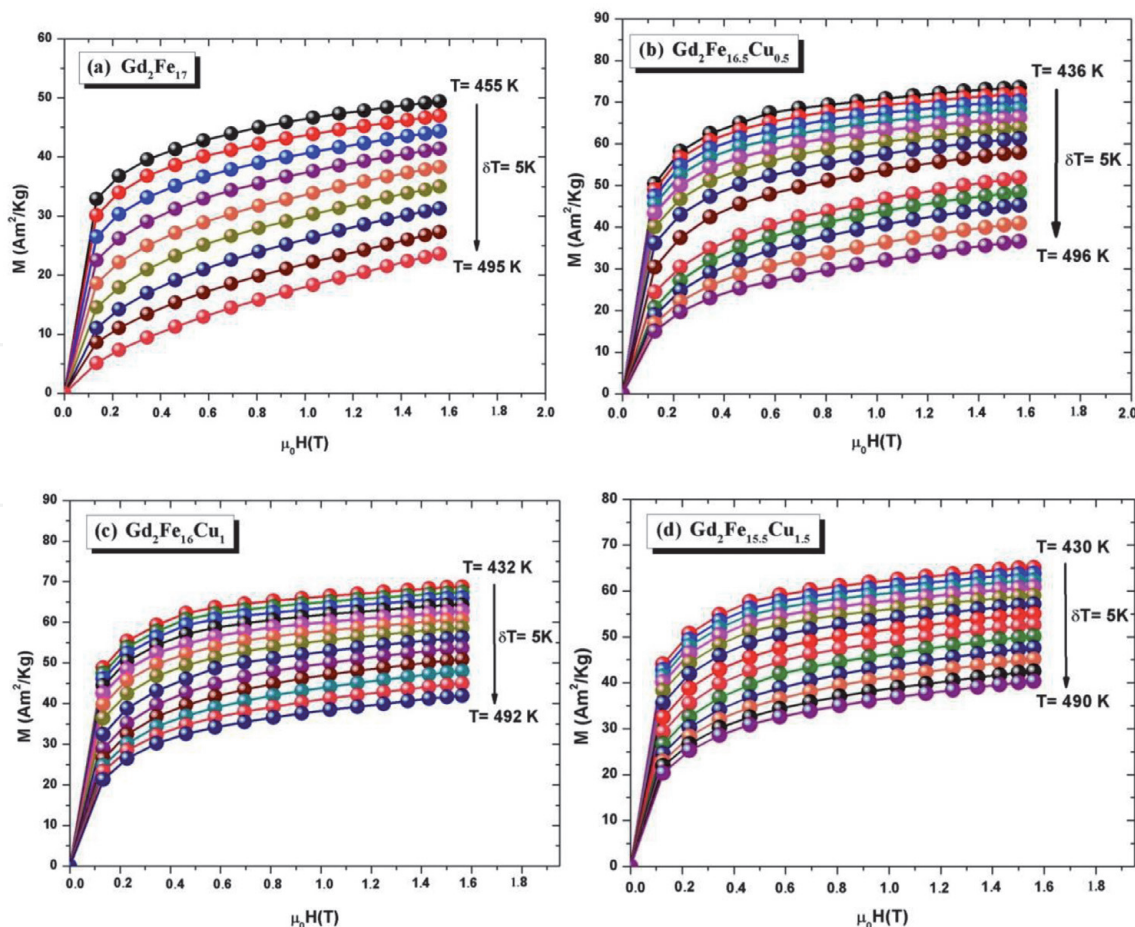


**Figure 15.**  
*Variations of the magnetization as a function of the magnetic field applied for the compounds  $Gd_2Fe_{17-x}Cu_x$  ( $x = 0; 0.5; 1$  et  $1.5$ ).*

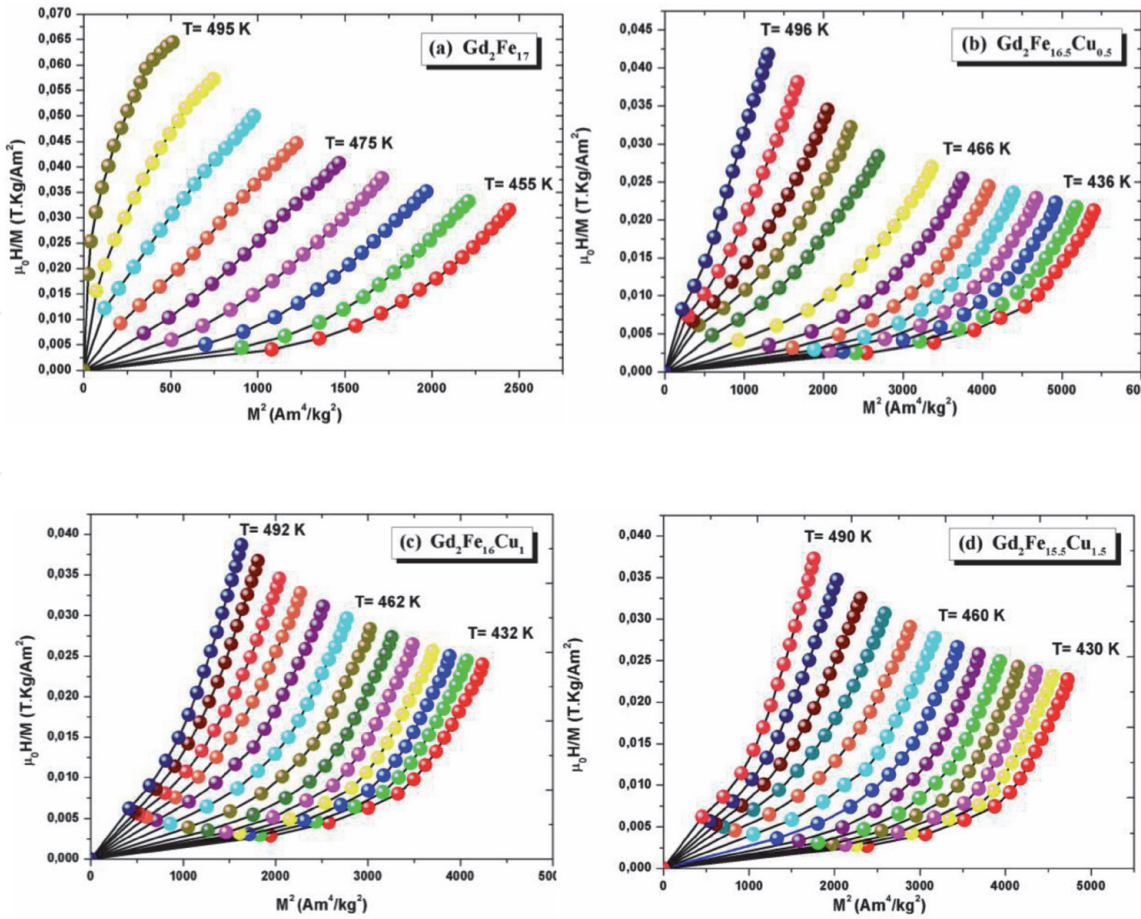


**Figure 16.**  
Arrott plots of compounds  $\text{Gd}_2\text{Fe}_{17-x}\text{Cu}_x$  ( $x = 0; 0.5; 1$  et  $1.5$ ).

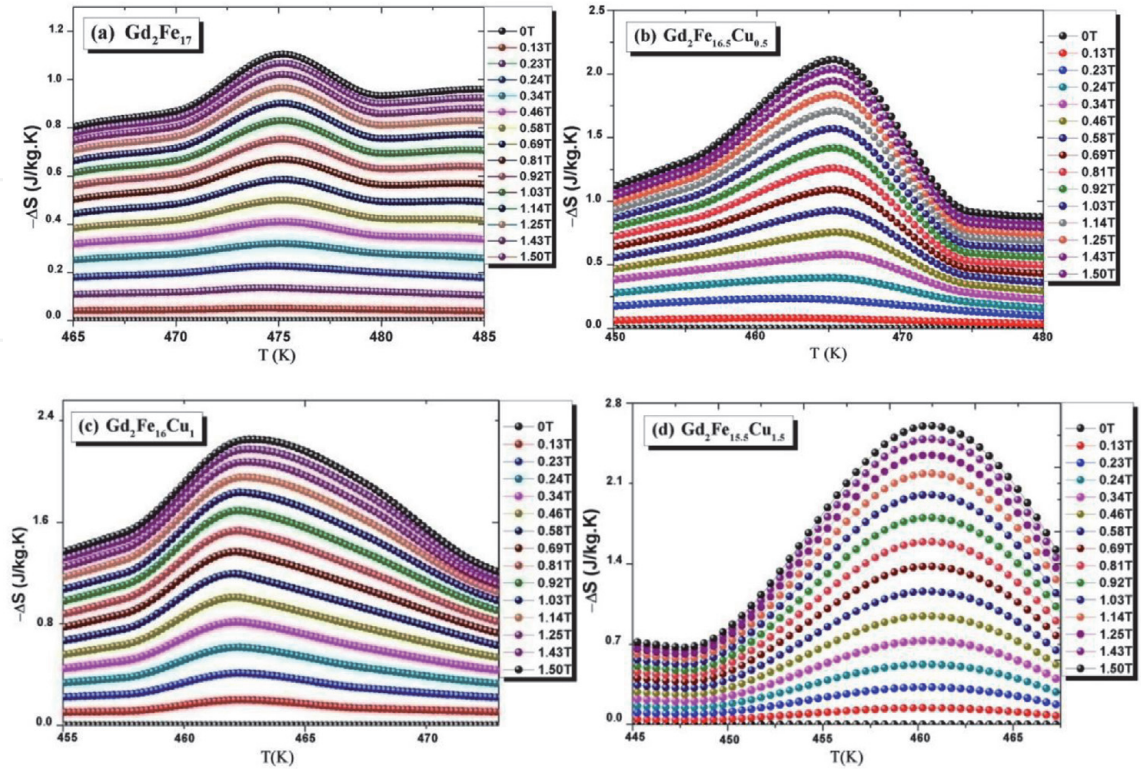


**Figure 17.**  
Variations in magnetic entropy as a function of temperature and the applied magnetic field of the  $\text{Gd}_2\text{Fe}_{17-x}\text{Cu}_x$  compounds ( $x = 0; 0.5; 1$  and  $1.5$ ).

## 7.2 Magnetocaloric effect of the $\text{Gd}_2\text{Fe}_{17-x}\text{Cu}_x$ series ( $0 \leq x \leq 1.5$ )

The variation in magnetic entropy ( $-\Delta S_{\text{Max}}$ ) as a function of temperature under different magnetic fields for  $\text{Gd}_2\text{Fe}_{17-x}\text{Cu}_x$  compounds ( $x = 0; 0.5; 1$  and  $1.5$ ) is shown in **Figure 17**. The curves show a maximum in the vicinity of the Curie temperature. It is found that the substitution of iron by copper causes an increase in the magnetocaloric effect. The values of the magnetic entropy of the  $\text{Gd}_2\text{Fe}_{17-x}\text{Cu}_x$  system are close to those determined in solid solutions  $\text{Pr}_2(\text{Fe}, \text{Al})_{17}$  and  $\text{Gd}_2(\text{Fe}, \text{Si})_{17}$  [59].

**Table 6** shows that the values of the maximum magnetic entropy and the cooling capacity (RCP) of the compounds in the solid solution  $\text{Gd}_2\text{Fe}_{17-x}\text{Cu}_x$  ( $0 \leq x \leq 1.5$ ) increase with the copper content.

| X   | 0    | 0.5  | 1    | 1.5  |
|---|------|------|------|------|
| $\Delta S_{\text{Max}} (\text{J} \cdot \text{kg}^{-1} \cdot \text{K}^{-1})$ | 1,14 | 2,14 | 2,35 | 2,54 |
| RCP ( $\text{J} \cdot \text{kg}^{-1}$ )                                     | 18   | 23,7 | 27,2 | 31,5 |

**Table 6.**

Magnetic entropy and cooling capacity of  $\text{Gd}_2\text{Fe}_{17-x}\text{Cu}_x$  compounds ( $x = 0; 0.5; 1$  and  $1.5$ ).

## 8. Conclusion

In summary, the structural characterization, determination of the magnetic properties and the magnetocaloric effects were performed for the  $\text{Nd}_2\text{Fe}_{17-x}\text{Co}_x$  ( $x = 0; 1; 2; 3$  and  $4$ ) and  $\text{Gd}_2\text{Fe}_{17-x}\text{Cu}_x$  ( $x = 0, 0.5, 1$  and  $1.5$ ) compounds. A single rhombohedral Th2Zn17 phase was obtained after one week of heat treatment at  $800^\circ\text{C}$  for synthesis by means of arc-melting. The crystal structure of the parent  $\text{R}_2\text{Fe}_{17}$  was found to remain unchanged for the  $\text{Gd}_2\text{Fe}_{17-x}\text{Cu}_x$  and  $\text{Sm}_2\text{Fe}_{17-x}\text{Ni}_x$  compounds which crystallize in the rhombohedral structure with the space group  $\bar{R}\bar{3}m$ . Knowledge of the Maxwell relationship is essential to understanding the behavior of magnetocaloric materials and they also serve as indicators in the search for ever better performing compounds. Thus, a lot of information is to be extracted:

The magnetization decreases as the temperature increases,  $(\partial M / \partial T) H < 0$ , so  $\Delta S_{\text{Max}}$  should be negative and this is well confirmed for our samples.

For ferromagnetic compounds, the maximum value of  $(\partial M / \partial T) H$  is reached at  $T_C$ , which means that the evolution of  $\Delta S_{\text{Max}}$  as a function of temperature describes a peak whose maximum is at  $T_C$ , which works well with the results found for our systems. In all the materials studied in the thesis, the behavior of  $\Delta S_{\text{Max}}$  gradually decreases on either side of the order temperature. The Curie temperature of  $\text{Nd}_2\text{Fe}_{17-x}\text{Co}_x$  ( $x = 0; 1; 2; 3$  and  $4$ ) compounds increases with Co content from 326 to 620 K for  $x = 0$  to  $x = 4$ , respectively. The Curie temperature is the result of two effects: a magneto-volumic effect linked to Fe-Fe distances and an electronic effect linked to the filling of the 3d band of iron. For the system studied, the volume of the mesh remains constant as a function of the degree of substitution of the cobalt, this shows that the electronic effect dominates the magneto-volume effect. The study of the magnetic properties shows the Curie temperature and the entropy variation  $\Delta S$  increase. This increase is explained by the Co-Co interactions which become stronger.

The experimental results show that in the  $\text{Gd}_2\text{Fe}_{17-x}\text{Cu}_x$  ( $x = 0, 0.5, 1$  and  $1.5$ ) compounds, the Curie temperature decreases by increasing the copper content from 475 K for ( $x = 0$ ) to 460 K for ( $x = 1.5$ ). This behavior can be attributed to the unit-cell volume decrease and the magnetic dilution. Moreover, we found that the copper substitution leads to an increase in  $\Delta S_{\text{Max}}$  from  $1.14 \text{ J/kg}$  for  $\text{Gd}_2\text{Fe}_{17}$  to  $2.54 \text{ J/kg K}$  for  $\text{Gd}_2\text{Fe}_{15.5}\text{Cu}_{1.5}$ .



### Author details

Mosbah Jemmal<sup>1,2\*</sup> and Lotfi Bessais<sup>3</sup>

1 LSME, Faculty of Science, University of Sfax, Sfax, Tunisia

2 Department of Chemistry, College of Science and Arts, Ar-rass, Qassim University, Buraydah, Saudi Arabia

3 Univ Paris Est Creteil, CNRS, ICMPE, Thiais, France

\*Address all correspondence to: jmosbah73@gmail.com



© 2021 The Author(s). Licensee IntechOpen. This chapter is distributed under the terms of the Creative Commons Attribution License (<http://creativecommons.org/licenses/by/3.0>), which permits unrestricted use, distribution, and reproduction in any medium, provided the original work is properly cited. CC BY

## References

- [1] V. K. Pecharsky, K. A. Gschneidner, Phys. Rev. Lett., 78 (1997) 4494.
- [2] V. K. Pecharsky, K. A. Gschneidner, J. Mag. Mag. Mat., 167 (1997) 179.
- [3] V. K. Pecharsky, K. A. Gschneidner, Phys. Lett., 70 (1997) 3299.
- [4] D. M. Dimiduk, Y. W. Kim, R. Wagner, M. Yamaguchi. TMS, Warrendale, (1995) 3.
- [5] N. S. Stolo, C. T. Liu, S. C. Deevi, Intermetallics., 8 (2000) 1313.
- [6] K. H. J. Buschow, Handbook of Magnetic Materials., 10 (1997) 463.
- [7] L. Bessais, C. Djega-Mariadassou, V. H. Ky, N. X. Phuc, J. Alloys Compd. 426 (2006) 22.
- [8] E. Burzo, A. Chelkovski, and H.R. Kirchmayr, Landolt-Bornstein Handbook (Berlin, 1990).
- [9] S. Chikazumi, Physics of Ferromagnetism, 2nd edn. (Oxford: Oxford University Press, 1997).
- [10] P.J. Clegg and L. Bessais, J. Magn. Magn. Mater., 202 (1999) 554.
- [11] D. Givord and R. Lemaire, IEEE Trans. Magn. , 10 (1974) 109.
- [12] K.H.J. Buschow, Rep. Prog. Phys., 40 (1977) 1179.
- [13] K.H.J. Bushow, Handbook of Magnetic Materials, vol. 4(Amsterdam: Elsevier, 1988).
- [14] E. Belorizky, M.A. Fremy, J.P. Gavigan, D. Givord, and H.S.Li, J. Appl. Phys., 61 (1987) 3971.
- [15] K.H.J. Buschow, Rep. Prog. Phys., 54 (1991) 1123.
- [16] J.J.M. Franse, R.J. Radwanski, and K. H.J. Buschow, Handb. Magn. Mater., 7 (1993) 307.
- [17] K.H.J. Buschow, Magnetism and Processing of Permanent Magnet, Volume 10 of Handbook of Magnetic Materials(Amsterdam: Elsevier, 1997).
- [18] J.X. Zhang, L. Bessais, C. Djega-Mariadassou, E. Leroy, and A. Percheron-Guegan, Appl. Phys. Lett., 80 (2002)1960.
- [19] L. Bessais, E. Dorolte, and C. Djega-Mariadassou, Appl. Phys. Lett., 87 (2005) 192503.
- [20] H. Chen, Y. Zhang, J. Han, H. Du, Ch. Wang, and Y. Yang, J. Magn. Magn. Mater. , 320 (2008) 1382.
- [21] P. Alvarez, P. Gorria, V. Franco, J.S. Marcos, M.J. Perez, J.L.S. Llamazares, I. P. Orench, and J.A. Blanco, J. Phys. Condens. Matter ,22 (2010) 216005.
- [22] P. Alvarez, P. Gorria, J.S. Marcos, J. L.S. Llamazares, and J.A. Blan, J. Phys. Condens. Matter 25, (2013) 496010.
- [23] R. Guetari, R. Bez, A. Belhadj, K. Zehani, A. Bezerghaneu, N. Mliki, L. Bessais, and C.B. Cizmas, J. Alloys Compd., 588 (2014) 64.
- [24] S. Charfeddine, K. Zehani, L. Bessais, and A. Korchef, J. Solid State Chem., 238 (2016) 15.
- [25] C. Djega-Mariadassou and L. Bessais, J. Magn. Magn. Mater. 210.
- [26] M. Saidi, S. Walha, K. Nouri, A. Kabadou, M. Jemmali, L. Bessais, Journal of Alloys and Compounds 781 (2019) 159.
- [27] N. Bouchaala, M. Jemmali, K. Nouri, S. Walha, A. BenSalah, L. Bessais, J. Phase Equilib. Diffus., 38 (2017) 561.

- [28] N. Bouchaala; M. Jemmali; T. Bartoli; K. Nouri; I. Hentech; S. Walha; A. Ben Salah; L . Bessais. Journal of Solid State Chemistry, 258 (2018) 501
- [29] M. Saidi, K. Nouri, S. Walha, E. Dhahri, A. Kabadou, M. Jemmali and L. Bessais, Journal of Electronic Materials, 48 (2019) 2242.
- [30] K. Nouri, M. Jemmali, S. Walha, K. Zehani, L. Bessais, A. Ben Salah J. Alloys Compd. 661 (2016) 508.
- [31] L. Bessais, C.D. Mariadassou, D.K. Tung, V.V. Hong, and N.X. Phuc.pp. J. Alloys Compd.,455 (2008) 35.
- [32] I. Nehdi, M. Abdellaoui, C. D. Mariadassou, L. Bessais, H. Zarrouk. Physical and Chemical News,13 (2003) 21.
- [33] C. Djéga.Mariadassou, L. Bessais, A. Nandra, J. M. Grenèche, E. Burzo. Phys. Rev. B,65 (2001) 14419.
- [34] I.A. Al.Omari, S.S. Jaswal, A.S. Fernando, D.J. Sellmyer. J. Appl. Phys., 76 (1994) 6159.
- [35] X.C. Kou, R. Grossinger, T.H. Jacobs, and K.H.J. Buschow. J. Magn. Magn. Mater., 88 (1990) 1.
- [36] M. Jemmali, S. Walha, M. Pasturel, O. Tougait, R. Ben Hassen, H. Noël. J. Alloys Compd., 489 (2010) 421.
- [37] M. Jemmali, S. Walha, , R. Ben Hassen, H. Noël. Asian Journal of Chemistry, 28 (2016), 1330.
- [38] Z. W. Li., X.Z. Zhou and A.H. Morrish, Phys. Rev. B, 51 (1995) 2891.
- [39] C. Lin, Y.X. Sun, Z.X. Liu, H.W. Jiang and Z. X. Liu, H.W. Jiang and Z. H. Liu, IEEE Trans. Magn., 28(1 992) 2844.
- [40] PhD thesis by A. Nandra, defense 2003, structural and magnetic study of nanocrystalline alloys  $\text{Sm}_2\text{Fe}_{17-x}\text{Si}_x$  and their non-equilibrium  $\text{SmFe}_{9-y}\text{Si}_y$  precursors, non-carburized and carburized.
- [41] Z.Y. Ren, W.Y.Lee, C.D. Qin, D.H. L. Ng and X.Y.Ma, J. Appl.Phys. , 85 (1999) 4672.
- [42] F.M. Yang, W Gong and G.C. Hadjipanayis, J. Appl.Phys. ,76 (1994) 6156.
- [43] D.M. Zhang, Y. H. Gao, B.M. Yu, C. Q. Tang, N. Tang, X.P. Zhong, W.C. Lin, F.M.Yang and F.R. de Boer, J. Appl. Phys. , 76 (1994) 7452.
- [44] E. Burzo, Solid State Commun, 89 (1994) 519.
- [45] P. Brommer, Physica B,154 (1989) 197.
- [46] H.Liu, D.Wang, S.Tang, Q. Cao, T. Tang, B. Gu, Y. Du, J. Alloys Compd. 346 (2002) 314.
- [47] X. B. Liu, Z. Altounian, J. Magn. Magn. Mater., 292 (2005) 83.
- [48] G. V. Brown, J. Appl. Phys., 47 (1976) 3673.
- [49] V. K. Pecharsky, K. A. Gschneidner. Jr, Phys. Rev. Let., 78 (1997) 4494.
- [50] D. Givord and R. Lemaire. IEEE Trans.Magn., MAG-10 (1974)109.
- [51] C. Djega-Mariadassou and L. Bessais. J.Magn.Magn.Mater., 210 (2000)81.
- [52] Z.W. Li and A. H.Morrish. Phys. Rev. B, 55(1997)3670.
- [53] B. G. Shen, F.W.Wang, H. Y. Gong, Z. H. Cheng, B. Liang, and J. X. Zhang. J. Phys. :Condens. Matter, 7 (1995) 883.
- [54] F. M. Yang, X.W. Li, N. Tang, J.L. Wang, Z. H. Lu, T. Y.Zhao, Q. A. Li, J. P.

Liu, and F. R. de Boer. J. Alloys Compd.,  
221 (1995)248.

[55] D. Givord and D. Courtois, J.Magn.  
Magn. Mater. , 196 (1999) 684.

[56] M.Z. Huang, W.Y.Ching and Z.Q.  
Gu J. Appl.Phys. , 81 (1997) 5112.

[57] A. M.Tishin, K. A. Gschneidner Jr.  
and V. K. Pecharsky. Phys. Rev. B, 59  
(1999) 503.

[58] H. Chen, Y.Zhang, J. Han, H. Du,  
Ch. Wang, Y.Yang.Journal of  
Magnetism and Magnetic Materials 320  
(2008) 1382.

[59] K. Zehani, R. Guetari, N. Mliki, L.  
Bessais. Physics Procedia, 75(2015) 1435